

pubs.acs.org/JPCB Article

# The Photoactive Excited State of the B<sub>12</sub>-Based Photoreceptor CarH

Nicholas A. Miller, April K. Kaneshiro, Arkaprabha Konar, 

Roberto Alonso-Mori, Alexander Britz, Aniruddha Deb, James M. Glownia, Jake D. Koralek, Leena Mallik, Joseph H. Meadows, Lindsay B. Michocki, Tim B. van Driel, Markos Koutmos, S. Padmanabhan, Montserrat Elías-Arnanz, Kevin J. Kubarych, E. Neil G. Marsh, James E. Penner-Hahn,\* and Roseanne J. Sension\*



Cite This: J. Phys. Chem. B 2020, 124, 10732-10738



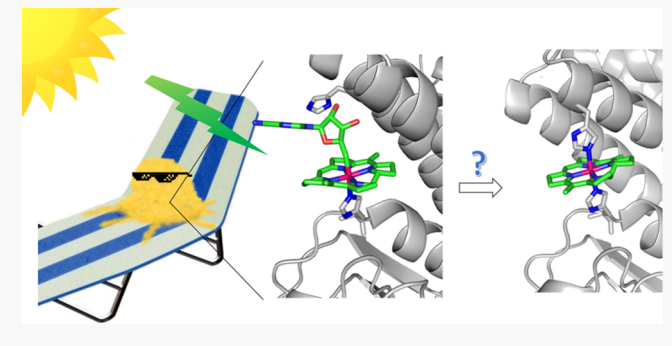
**ACCESS** 

III Metrics & More

Article Recommendations

Supporting Information

ABSTRACT: We have used transient absorption spectroscopy in the UV-visible and X-ray regions to characterize the excited state of CarH, a protein photoreceptor that uses a form of B<sub>12</sub>, adenosylcobalamin (AdoCbl), to sense light. With visible excitation, a nanosecond-lifetime photoactive excited state is formed with unit quantum yield. The time-resolved X-ray absorption near edge structure difference spectrum of this state demonstrates that the excited state of AdoCbl in CarH undergoes only modest structural expansion around the central cobalt, a behavior similar to that observed for methylcobalamin rather than for AdoCbl free in solution. We propose a new mechanism for CarH photoreactivity involving formation of a triplet excited state.



This allows the sensor to operate with high quantum efficiency and without formation of potentially dangerous side products. By stabilizing the excited electronic state, CarH controls reactivity of AdoCbl and enables slow reactions that yield nonreactive products and bypass bond homolysis and reactive radical species formation.

## ■ INTRODUCTION

Light provides a versatile energy source capable of precise manipulation of material systems on size scales ranging from molecular to macroscopic. Natural biological systems use light as an energy source in sensing and feedback. Examples of lightresponsive sensors used to produce action in biological systems range broadly from the well-studied rhodopsins to the newly discovered B<sub>12</sub>-dependent CarH photoreceptor family that is widespread in bacteria. 1-9 CarH functions as a transcription factor, whose activity is modulated by changes of its oligomeric state through the interaction with 5'-deoxyadenosylcobalamin (AdoCbl, coenzyme B<sub>12</sub>) and light. In CarH (Thermus thermophilus), photoexcitation of AdoCbl triggers dissociation of its upper axial 5'-deoxyadenosyl group, which is replaced with a histidine ligand to form a bis-His cobalamin (Figure 1, see also Figure S1). This event initiates a structural change in the protein-DNA complex that releases DNA for transcription, 7,10 thereby up-regulating the carotenoid biosynthesis and protecting the organism from photooxidative damage.

The use of AdoCbl as the photosensor in CarH is surprising and intriguing. Optical excitation of AdoCbl, whether free or protein-bound, normally results in the homolytic cleavage of the Co–C bond, with rapid formation of cob(II)alamin and an extremely reactive adenosyl radical. Such reactivity in CarH would risk both the occurrence of unwanted side reactions promoted by radical formation and the potential

destruction of a biosynthetically expensive cofactor. It is thus paradoxical that a cell response meant to mitigate photooxidative damage by highly reactive oxygen species (ROS) would rely on a photoreceptor that uses AdoCbl to sense light and generate another equally reactive radical species, which itself can cause cellular damage or propagate the production of ROS. Consequently, the biological use of CarH must rely on some mechanism to countervail such damaging radical reactions in vivo. Indeed, CarH alters the photolysis of its bound AdoCbl to avoid the release of adenosyl radicals by generating instead nonreactive 4',5'-anhydroadenosine (Figure 1), a product never previously detected upon AdoCbl photolysis.<sup>7,17</sup> The mechanistic basis for this photochemical reaction remains elusive. Thus, how CarH channels light energy in a productive direction and prevents damage that could be caused by unfettered radical formation remains one of the key questions for understanding this photosensor. 17-22

The UV-visible spectra for AdoCbl bound to CarH, for AdoCbl bound to glutamate mutase (Glm), for protein-free

Received: October 18, 2020 Published: November 11, 2020





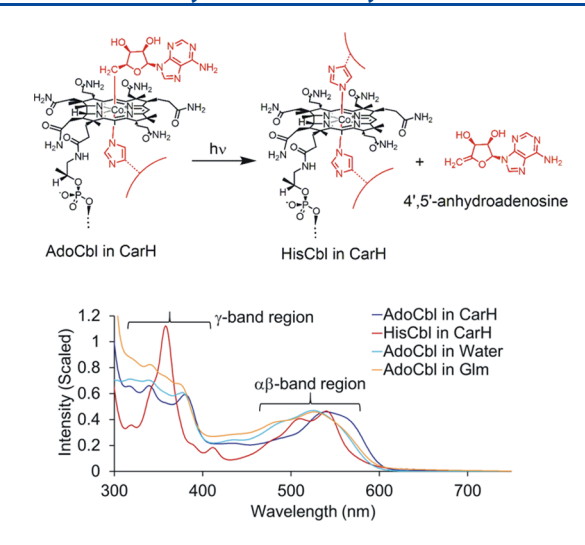


Figure 1. (top) Schematics of adenosylcobalamin (AdoCbl) bound to CarH and the bis-His photoproduct and 4′,5′-anhydroadenosine product of CarH-bound AdoCbl photolysis. When AdoCbl binds CarH, the lower axial ligand of the central cobalt (5,6-dimethylbenzimidazole) is displaced by a conserved histidine (the base-off/His-on mode). (bottom) UV—visible spectra of AdoCbl bound to CarH, free in solution, and bound to glutamate mutase (Glm) and the light stable photoproduct in CarH (HisCbl).

AdoCbl in water, and for the HisCbl photoproduct of CarH are plotted in Figure 1. This comparison clearly shows that CarH perturbs the low-lying valence electronic states of AdoCbl. The spectra of AdoCbl in water and in Glm are similar, while the  $\alpha\beta$ -band of AdoCbl in CarH is strongly redshifted. The protein also perturbs the orientation of the 5'deoxyadenosyl group of AdoCbl in CarH from that observed in crystals of free AdoCbl (see Figure S1). 20,23 The available crystal structure of Glm with AdoCbl bound does not have an intact Co-C bond, preventing direct comparison of the 5'deoxyadenosyl orientation in this protein.<sup>24</sup> Although the redshift of the spectrum in CarH is significant, the influence of the protein on the regions of the potential surface away from the vertical Franck-Condon region is of more importance for the photochemistry of AdoCbl; transient spectroscopies permit us to probe these regions of the excited electronic state. A visible transient absorption measurement by Kutta et al. used near UV excitation at 370 nm to investigate the initial excitedstate dynamics, suggesting a low quantum yield for the photochemical activity of AdoCbl bound to CarH and a novel mechanism.<sup>18</sup> However, the photochemistry of cobalamins is known to be wavelength-dependent in some cases.<sup>25–28</sup> Here, we use ultrafast UV-visible spectroscopy to characterize the excited electronic state of AdoCbl bound to Thermus thermophilus CarH following 520 to 565 nm excitation (in the visible  $\alpha\beta$ -band region of the spectrum) and combine these measurements with transient X-ray absorption near edge structure (XANES) spectra to probe the changes in excitedstate structure more directly.

## **■ EXPERIMENTAL METHODS**

CarH was expressed, purified, and concentrated using previously published procedures. CarH samples were filtered with 0.22  $\mu$ m syringe filters to remove aggregates. The concentration and sample integrity were confirmed by steady-state UV—visible spectroscopy to ensure that all the coenzyme was bound. The coenzyme concentration was ~250

 $\mu M$  for the UV experiment and ~200  $\mu M$  for the visible experiment. For XANES measurements, the coenzyme concentration was ~200  $\mu M$ , and a small amount of glycerol was added to the solution to stabilize droplet formation. After UV-visible transient absorption experiments, the irradiated CarH samples were filtered with a 0.22  $\mu m$  syringe filter, and their spectra were collected. This filtered solution of the CarH photoproduct was then used for the photoproduct transient absorption (see Figure S2).

Transient absorption measurements were performed using the LUMOS pump-probe instrument. The first experiment used 500 nJ, 550 nm excitation pulses with a 10 nJ supercontinuum generated by focusing the second harmonic 400 nm into a translating CaF<sub>2</sub> window. The continuum covered the range from 280 to 350 nm and 440 to 515 nm. The region from 350 to 440 nm was blocked with a filter to eliminate a strong 400 nm residual. The second experiment used 250 nJ, 565 nm excitation pulses with a 10 nJ supercontinuum probe generated by focusing the 800 nm fundamental into a translating CaF2 window. In this case, the continuum spanned the region from 330 to 725 nm. For both experiments, foci of excitation and detection beams were nominally 100  $\mu$ m full width at half maximum (FWHM), and the relative polarization was set at magic angle. The extinction coefficient difference between CarH and the photoproduct reaches a maximum at 565 nm. This excitation wavelength was used for the second measurement to minimize the contribution of the photoproduct to transient absorbance measurements.

Transient absorption measurements were performed using a small volume flow system requiring about 3 mL of solution recirculated through a 2 mm path length flow cell. Transient absorption measurements of coenzyme B<sub>12</sub> (AdoCbl) in buffer solution were performed before and after the CarH transient absorption experiments to ensure that laser alignment and/or drift did not affect the results. These measurements agreed with extensive prior measurements on AdoCbl. To ensure the integrity of the data, 70 time delays were chosen to limit each scan to 2 min. Difference spectra were computed from 500 pump-on and 500 pump-off shots. Sequential scans were compared to ensure that photoproduct buildup was not distorting the signal. Two data sets were combined for analysis and plotting using the regions of overlap from 330 to 350 nm and 440 to 515 nm. The difference spectra obtained for the light stable CarH photoproduct (Figure S2) in the UV region demonstrate that photoproduct buildup is minimal and makes no significant contribution to the CarH difference spectrum in Figure 2. A transient absorption spectrum of MeCbl was also obtained for comparison with the CarH excited-state spectrum. These data are consistent with previous measurements.

The transient XANES spectrum of AdoCbl bound to CarH was measured using the XPP instrument at LCLS (Linac Coherent Light Source). The time delay was set at  $\sim\!40$  ps between optical excitation and X-ray probe pulses. The excitation wavelength was 520 nm, chosen to optimize overlap with the UV–visible spectra of a range of cobalamins during the LCLS run. The relative polarization was set to perpendicular to maximize the magnitude of the signal. The drop delivery system used for the CarH measurements and the method for analyzing the data to correct for variable drop size have been described previously. The CarH sample was ca. 0.2 mM with 5% glycerol added to the buffer solution to stabilize the droplet formation. The droplet size was  $\sim\!55~\mu{\rm m}$  in diameter. The average hit rate, where the X-ray laser pulse

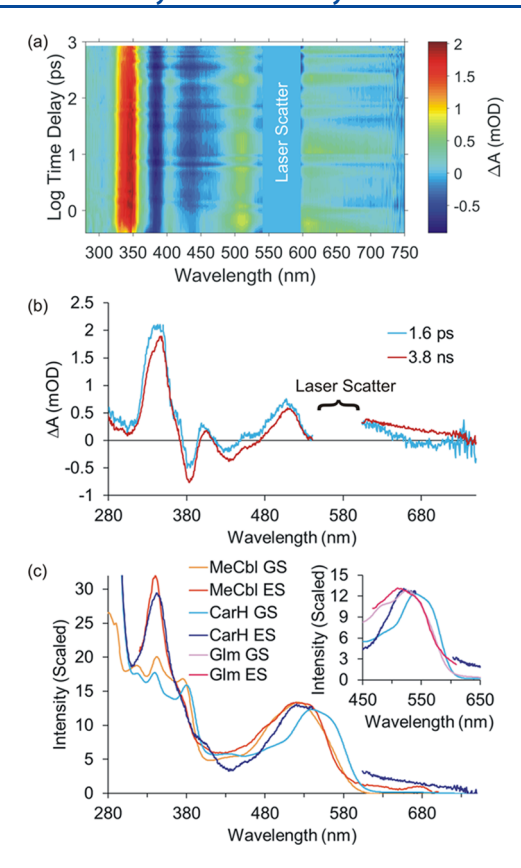


**Figure 2.** UV—visible transient difference spectra following excitation of AdoCbl bound to CarH. (a) Log plot of the transient difference spectrum from 400 fs to 850 ps. The region from 540 to 597 nm, which is dominated by scatter from the pump pulse, is omitted. Kinetic traces at selected wavelengths are included in Figure S3. Spectra at selected time delays are included in Figure S4. (b) Species-associated difference spectra determined from the fit to the data. (c) Ground-state (GS) and estimated excited-state (ES) spectra of MeCbl<sup>27,35,36</sup> in solution and AdoCbl bound to CarH. The inset compares the ground- and excited-state spectra of AdoCbl bound to CarH with AdoCbl bound to Glm. <sup>11,12</sup> See Figure S5 for excited-state spectra of AdoCbl free in solution and for a comparison of the estimated excited-state spectra of both components plotted in (b).

and droplet overlapped in time and space, was 44 to 48%. See  $ref^{30}$  for more details.

The asterisks in Figure 3 and the open circles in Figure S6 indicate regions where artifacts are observed in the CarH XANES spectra. These were observed in all measurements on all samples during the run at LCLS, with a relative intensity that depends on the magnitude of solute fluorescence. These are independent of the optical laser and cancel out in the difference spectrum.

Comparison measurements of MeCbl in aqueous solution at 100 ps<sup>31</sup> and AdoCbl in water and in ethylene glycol at 1 to 2 ps<sup>32</sup> were performed using a liquid jet sample delivery system and sample concentrations of ca. 5 mM. All plots compare the difference spectra obtained with perpendicular polarization of the X-ray and optical pulses to the results obtained for CarH with the same polarization geometry.

## RESULTS

The transient UV—visible absorption spectra of AdoCbl bound to CarH following excitation at 565 nm are plotted in Figure 2a. Photoproduct buildup is a potential complication in CarH

studies. A separate transient absorption measurement of the light stable bis-His CarH photoproduct probing the UV region (Figure S2) confirms the result of Kutta et al. 18 that this species undergoes internal conversion to the ground state on a ca. 3.7 ps timescale without formation of a photoproduct. Photoproduct buildup is minimal in our measurements using rapid scans and a flow cell, and the product makes no significant contribution to the difference spectrum of AdoCbl bound to CarH in Figure 2.

The data in Figure 2a were fit to a biexponential decay yielding a fast 1.6 ps relaxation component and an extremely slow decay of ca. 3.8 ns. The protein active site thus stabilizes an electronic excited state that is formed with near unit quantum yield and that persists for nanoseconds. The species-associated difference spectra of the initial state and the metastable excited state of AdoCbl bound to CarH are plotted in Figure 2b. The comparison of the 1.6 ps and 3.8 ns components demonstrates that there is only a slight redshift of the transient spectrum over time. These difference spectra match neither the cob(II)alamin-CarH nor the photoproduct-CarH difference spectra. This suggests that in contrast with AdoCbl in other environments that in contrast with AdoCbl in other environments and with other alkylcobalamins, 27,28,33-35 there is no evidence for bond cleavage in CarH during at least the first few nanoseconds following visible light excitation.

The excited electronic states of the two biologically relevant forms of B<sub>12</sub>, AdoCbl and methylcobalamin (MeCbl, which has a methyl group as the upper axial ligand) have been extensively investigated using UV-visible, 8,11-14,18,27,28,34,35,37 transient absorption spectroscopy. Kutta et al. used femtosecond transient absorption spectroscopy with excitation at 370 nm to show that the AdoCbl in CarH branches between several distinct processes including fast internal conversion to the ground state ( $\varphi_{\rm IC} \approx$  0.9), homolysis of the Co–C bond ( $\varphi_{\rm Hom}$  $\approx$  0.02), and formation of a metastable cob(III)alamin-like metal-to-ligand charge transfer (MLCT) excited state ( $\varphi_{ES} \approx$ 0.08). They suggested that the low yield of the photoactive state provided a strategy for limiting response to light and avoiding the overproduction of carotenoids. 18 In contrast, our results demonstrate that excitation in the visible region of the spectrum, which better matches the intensity of solar radiation reaching the earth's surface, avoids prompt dissociation and internal conversion and instead produces the metastable cob(III)alamin-like excited state identified by Kutta et al. in

Interpretation of the optical difference spectrum is not intuitive because it depends on both the ground- and excitedstate absorption spectra. The excited-state spectrum may be estimated by adding a scaled amount of the ground-state spectrum to the difference spectrum, providing a more intuitive comparison between compounds. In Figure 2c, we compare the estimated excited-state spectra of MeCbl<sup>27,35,36</sup> and CarH. The excited-state spectra are similar in both the appearance of a strong  $\gamma$ -band at 338 nm and in the shape of the visible  $\alpha\beta$ band around 500 nm, although the  $\alpha\beta$ -band of CarH shows a small redshift relative to MeCbl. This shift is smaller than the ground-state shift but still detectable. As noted by Kutta et al., both of these excited-state spectra are similar in the visible region to the spectrum of the 100 ps intermediate observed in glutamate mutase that precedes bond homolysis. 11,12 The similarity of the UV-visible transient absorption spectra suggests that the protein environment in CarH stabilizes for several nanoseconds an excited-state structure for the bound

AdoCbl that is similar to the excited state of free MeCbl and of AdoCbl bound to Glm, albeit with a much longer lifetime.

In order to explore the structure of this electronic excited state more directly, the transient XANES difference spectrum was measured at the cobalt K-edge for a time delay of 40 ps following excitation and compared with XANES measurements on other cobalamins. The sample was delivered as 55  $\mu$ m droplets synchronized with the X-ray and optical lasers, allowing measurement on samples only available in small volumes. The sample concentration (0.2 mM) was more than an order of magnitude lower than previous ultrafast XAS measurements on proteins on proteins or on liquid solutions. The ground-state XANES spectrum and excited-state transient difference spectrum of AdoCbl bound to CarH are compared with measurements on AdoCbl and of MeCbl in solution in Figure 3.

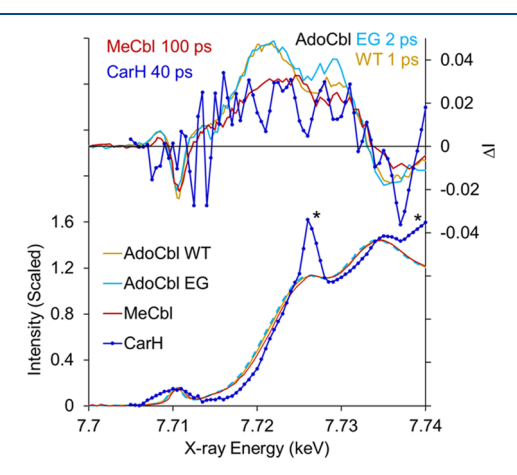


Figure 3. Ground-state XANES (below) and transient difference spectra (above) observed following excitation of AdoCbl in water (WT), in ethylene glycol (EG), and bound to CarH and of MeCbl in water. The time delays for the difference spectra are as indicated in the legend. The asterisks indicate regions where artifacts are observed in the CarH XANES spectra. These are independent of the optical laser and cancel out in the difference spectrum. The same scale factor is used for both the ground-state spectra and the difference spectra. Thus, the magnitude of the difference is consistent across all samples.

The ground-state spectra are all quite similar, consistent with the presence of similar alkyl ligation and similar bond lengths in each case.<sup>20,23</sup> The slightly higher energy of the CarH edge compared to the other three suggests that the average Coligand distance may be slightly shorter in CarH. Note, however, that the blueshift is much smaller than for cyanocobalamin (CNCbl, with a cyanide upper axial ligand), where the average axial bond length is significantly shorter ( $\sim$ 1.95 Å rather than  $\sim$ 2.1 Å, see Figure S6). The magnitudes of the difference spectra between the ground and excited states are similarly consistent for all four measurements. The right yaxis is expanded by a factor of ~17 compared with the scale for the ground-state spectra (left y-axis). Although the low signalto-noise ratio of the CarH data precludes detailed analysis, it is clear that the excited state does not involve extensive expansion of the axial bonds. If there was significant axial elongation, then the XANES difference signal would be much larger, as seen for example in CNCbl (Figure S6). 30,44,45 The difference spectra that are observed for the MeCbl excited state free in solution and the AdoCbl excited state in CarH are similar in both shape and magnitude, suggesting that the

structural changes around the cobalt are similar for both molecules, consistent with the UV-visible excited-state spectra.

In contrast to MeCbl and AdoCbl bound to CarH, the difference spectra for AdoCbl free in solution exhibit a larger redshift, as evidenced by the larger difference amplitude at ~7.720 keV. Polarization-resolved data for free AdoCbl in solution<sup>32</sup> and for MeCbl<sup>31</sup> have shown that the dominant contribution to the edge-shift is polarized out of the plane of the corrin ring, indicating changes in the axial bonds to the cobalt. The dominant contribution around 7.729 keV is polarized in the corrin ring reflecting changes in the equatorial bonds to the cobalt.<sup>31,32</sup> The differences between AdoCbl bound to CarH and free in solution suggest that the CarH protein inhibits bond elongation, while the overall similarity with MeCbl and with a higher energy region for AdoCbl in solution suggests that the dominant structural changes between the ground and excited state of AdoCbl bound to CarH are in the corrin ring.

#### DISCUSSION

Taken together, the UV-visible and XANES difference spectra demonstrate that the excited state of AdoCbl bound to CarH resembles the excited state of MeCbl rather than that of AdoCbl free in solution. While the spectral signatures of the excited state of MeCbl in solution and of the excited states of AdoCbl bound to CarH or Glm are similar, the fate of the electronically excited molecule differs (see Figure S7). In MeCbl, this state decays on a 1 ns timescale, branching between bond homolysis (15%) and internal conversion to the ground state (85%). 27,35,36 For AdoCbl bound to Glm, this state decays via bond homolysis on a timescale of  $105 \pm 10$  ps followed by geminate recombination accounting for 95% of the population. 11,12 The remaining 5% produces long-lived radicals. In contrast, the spectroscopically similar excited state of AdoCbl bound to CarH persists for nanoseconds, and its lifetime increases more than tenfold compared to that of Glm, with no evidence of internal conversion or ground-state

The challenge for the CarH protein is how to direct the photoreactivity of the AdoCbl cofactor so that the adenosyl ligand can dissociate and form 4′,5′-anhydroadenosine. The former allows coordination by an upper axial His132 and the consequent conformational change leading to its release from DNA to initiate transcription, while the latter avoids formation of highly reactive adenosyl radicals. The nature of the excited-state potential energy surface controls this reactivity. The protein environment in CarH and to a lesser extent in Glm stabilizes an excited-state structure with modest changes in the axial bonds. It is likely that the differing placement of the adenosyl group in CarH and the electrostatic environment provided by the protein serve to control the reactivity of the excited state (Figure 4 and Figure S8). A6,47

Transient measurements by Kutta et al. demonstrated formation of a second intermediate on the nanosecond timescale with a spectrum qualitatively similar to that of the initial excited state. <sup>18</sup> It was suggested that CarH altered the established photochemistry of bound AdoCbl by favoring heterolytic Co–C bond cleavage, thus bypassing the formation of an adenosyl radical and preventing the release of any radical generated by Co–C homolytic cleavage. We suggest instead that the long-lived state, designated D\* by Kutta et al. (Figure 5), results from an intersystem crossing to a six-coordinate

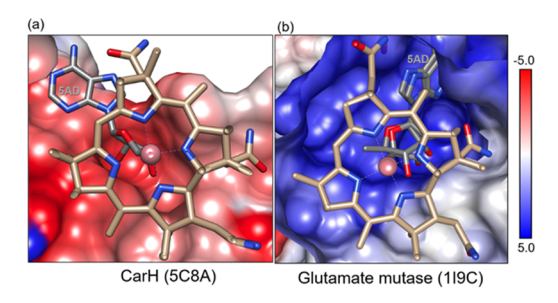


**Figure 4.** Electrostatic potential distribution at the substrate binding site of CarH (PDB ID, 5C8A) and glutamate mutase (PDB ID, 1I9C), computed by the Delphi web server.  $^{46,47}$  (a) CarH and (b) glutamate mutase bound to AdoCbl. Proteins are displayed with surface representations indicating the electrostatic distribution, while AdoCbl is represented as sticks. An expanded view of the binding pocket is shown in Figure S8. The electrostatic potential value ranges from -5kT/e (red) to 5kT/e (blue).

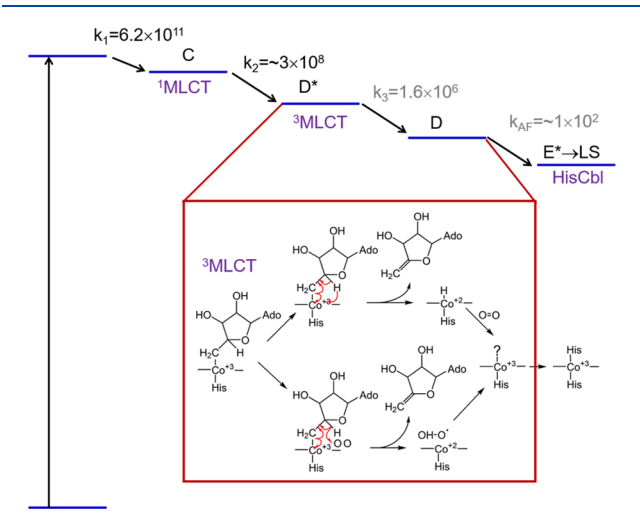


Figure 5. Proposed scheme for CarH photoreactivity.  $k_1$  and  $k_2$  are from this work;  $k_3$  and  $k_{\rm AF}$  are from Kutta et al. <sup>18</sup> In this scheme, the initial <sup>1</sup>MLCT state decays on the ns timescale to a <sup>3</sup>MLCT state (see text). We propose that this undergoes homolytic cleavage, either  $O_2$  promoted (lower pathway in the inset) or spontaneously (upper pathway, giving a cobalt hydride that would then react rapidly with  $O_2$ ). Either pathway would give a Co(III) cobalamin species on the microsecond timescale as observed by Kutta et al. <sup>18</sup> and the 4′,5′-anhydroadenosine product identified by Jost et al. <sup>17</sup> Such a species, whose axial ligation is at present not well-defined, would subsequently form the His-ligated CarH on a ms timescale. Intermediates are identified in purple with the corresponding letter labels from Kutta et al. also shown for each state (LS: light stable state).

triplet state since heterolysis would be expected to give larger differences in the UV—visible spectrum. A triplet excited state formed in this way could then persist for microseconds, providing time for excited-state reactions to form the stable 4′,5′-anhydroadenosine product<sup>17</sup> together with formation of the biologically relevant HisCbl photoproduct. Formation of a radical pair from the triplet state may also inhibit geminate recombination to the ground state and increase the quantum efficiency of the photoreceptor. We propose that the long lifetime of the initial <sup>1</sup>MLCT state allows CarH to form a triplet state that ultimately reacts to give stable products rather than geminate recombination or reactive radicals.

## CONCLUSION

The transient optical and X-ray measurements reported here demonstrate that the protein (CarH) controls reactivity of AdoCbl by stabilizing the excited electronic state and preventing the expansion of the axial bonds. This harnesses photon energy in the AdoCbl excited state to enable slow reactions including triplet formation and a reaction to form the stable 4',5'anhydroadenosine product rather than bond homolysis and the reactive 5'-deoxyadenosyl radical.

### ASSOCIATED CONTENT

## **5** Supporting Information

The Supporting Information is available free of charge at https://pubs.acs.org/doi/10.1021/acs.jpcb.0c09428.

Additional figures illustrating the experimental data, the structure of AdoCbl, the AdoCbl binding pocket, and reaction schemes (PDF)

### AUTHOR INFORMATION

## **Corresponding Authors**

James E. Penner-Hahn — Department of Chemistry and Department of Biophysics, University of Michigan, Ann Arbor, Michigan 48109-1055, United States; oorcid.org/0000-0003-0314-1274; Phone: +734-764-7324; Email: jeph@umich.edu

Roseanne J. Sension — Department of Chemistry, Department of Physics, and Department of Biophysics, University of Michigan, Ann Arbor, Michigan 48109-1055, United States; orcid.org/0000-0001-6758-0132; Phone: +734-764-6074; Email: rsension@umich.edu

# **Authors**

Nicholas A. Miller — Department of Chemistry, University of Michigan, Ann Arbor, Michigan 48109-1055, United States; orcid.org/0000-0002-9146-5414

April K. Kaneshiro – Department of Biological Chemistry, University of Michigan, Ann Arbor, Michigan 48109-0600, United States

Arkaprabha Konar — Department of Physics, University of Michigan, Ann Arbor, Michigan 48109-1040, United States; orcid.org/0000-0001-6546-4111

Roberto Alonso-Mori – Linac Coherent Light Source, SLAC National Accelerator Laboratory, Menlo Park, California 94025, United States

Alexander Britz — Linac Coherent Light Source and Stanford PULSE Institute, SLAC National Accelerator Laboratory, Menlo Park, California 94025, United States; orcid.org/0000-0002-1049-2841

Aniruddha Deb — Department of Chemistry and Department of Biophysics, University of Michigan, Ann Arbor, Michigan 48109-1055, United States; orcid.org/0000-0002-0331-9709

James M. Glownia – Linac Coherent Light Source, SLAC National Accelerator Laboratory, Menlo Park, California 94025, United States

Jake D. Koralek – Linac Coherent Light Source, SLAC National Accelerator Laboratory, Menlo Park, California 94025, United States

Leena Mallik – Department of Chemistry, University of Michigan, Ann Arbor, Michigan 48109-1055, United States Joseph H. Meadows – Department of Chemistry, University of Michigan, Ann Arbor, Michigan 48109-1055, United States

- Lindsay B. Michocki Department of Chemistry, University of Michigan, Ann Arbor, Michigan 48109-1055, United States
- Tim B. van Driel Linac Coherent Light Source, SLAC National Accelerator Laboratory, Menlo Park, California 94025, United States
- Markos Koutmos Department of Chemistry and Department of Biophysics, University of Michigan, Ann Arbor, Michigan 48109-1055, United States
- S. Padmanabhan Instituto de Química Física "Rocasolano", Consejo Superior de Investigaciones Científicas, Madrid 28006, Spain
- Montserrat Elías-Arnanz Departamento de Genética y Microbiología, Área de Genética (Unidad Asociada al Instituto de Química Física "Rocasolano", Consejo Superior de Investigaciones Científicas), Facultad de Biología, Universidad de Murcia, Murcia 30100, Spain
- Kevin J. Kubarych Department of Chemistry, University of Michigan, Ann Arbor, Michigan 48109-1055, United States; orcid.org/0000-0003-1152-4734
- E. Neil G. Marsh Department of Chemistry, University of Michigan, Ann Arbor, Michigan 48109-1055, United States; orcid.org/0000-0003-1713-1683

Complete contact information is available at: https://pubs.acs.org/10.1021/acs.jpcb.0c09428

## **Author Contributions**

◆Department of Chemistry and Biochemistry, Kent State University, 114 Science Research Building, Kent, Ohio 44242, United States (A.K.).

#### Notes

The authors declare no competing financial interest.

# ACKNOWLEDGMENTS

We thank Dr. Daniel P. DePonte for his insights and assistance on the drop delivery system for XANES measurements and Taylor E. McClain and Dr. Danielle Sofferman for the broadband transient UV-visible measurement of the MeCbl excited state. This work was supported by grants from the National Science Foundation NSF-CHE 1464584 and NSF-CHE 1836435 to R.J.S., NSF-CHE 1565795 to K.J.K., NSF-CHE 1608553 and NSF-CHE-1904759 to E.N.G.M., and NSF-CHE 1945174 to M.K.; from the Agencia Estatal de Investigación (AEI)-Spain and the European Regional Development Fund (FEDER) grants PGC2018-094635-B-C21 (to M.E.-A.) and PGC2018-094635-B-C22 (to S.P.); and from the Fundación Séneca (Murcia)-Spain grant 20992/PI/ 18 (to M.E.-A.). Portions of this work were carried out in the Laboratory for Ultrafast Multidimensional Optical Spectroscopy (LUMOS) supported by NSF-CHE 1428479. Use of the Linac Coherent Light Source (LCLS), SLAC National Accelerator Laboratory, is supported by the U.S. Department of Energy, Office of Science, Office of Basic Energy Sciences under contract no. DE-AC02-76SF00515.

### REFERENCES

- (1) Wickstrand, C.; Nogly, P.; Nango, E.; Iwata, S.; Standfuss, J.; Neutze, R. Bacteriorhodopsin: Structural insights revealed using X-ray lasers and synchrotron radiation. *Annu. Rev. Biochem.* **2019**, 88, 59–83.
- (2) Mansouri, M.; Strittmatter, T.; Fussenegger, M. Light-controlled mammalian cells and their therapeutic applications in synthetic biology. *Adv. Sci.* **2019**, *6*, 1800952.

- (3) Kottke, T.; Xie, A.; Larsen, D. S.; Hoff, W. D. Photoreceptors take charge: Emerging principles for light sensing. *Annu. Rev. Biophys.* **2018**, *47*, 291–313.
- (4) Govorunova, E. G.; Sineshchekov, O. A.; Li, H.; Spudich, J. L. Microbial rhodopsins: Diversity, mechanisms, and optogenetic applications. *Annu. Rev. Biochem.* **2017**, *86*, 845–872.
- (5) Losi, A.; Gardner, K. H.; Möglich, A. Blue-light receptors for optogenetics. *Chem. Rev.* **2018**, *118*, 10659–10709.
- (6) Meyer, T. E.; Kyndt, J. A.; Memmi, S.; Moser, T.; Colón-Acevedo, B.; Devreese, B.; Van Beeumen, J. J. The growing family of photoactive yellow proteins and their presumed functional roles. *Photochem. Photobiol. Sci.* **2012**, *11*, 1495–1514.
- (7) Padmanabhan, S.; Jost, M.; Drennan, C. L.; Elías-Arnanz, M. A new facet of vitamin B<sub>12</sub>: Gene regulation by cobalamin-based photoreceptors. *Annu. Rev. Biochem.* **2017**, *86*, 485–514.
- (8) Jones, A. R. The photochemistry and photobiology of vitamin  $B_{12}$ . *Photochem. Photobiol. Sci.* **2017**, *16*, 820–834.
- (9) Chemaly, S. M. New light on vitamin B<sub>12</sub>: The adenosylcobalamin-dependent photoreceptor protein CarH. S. Afr. J. Sci. **2016**, Volume 112, 39–47.
- (10) Ortiz-Guerrero, J. M.; Polanco, M. C.; Murillo, F. J.; Padmanabhan, S.; Elias-Arnanz, M. Light-dependent gene regulation by a coenzyme B<sub>12</sub>-based photoreceptor. *Proc. Natl. Acad. Sci. U. S. A.* **2011**, *108*, 7565–7570.
- (11) Sension, R. J.; Harris, D. A.; Stickrath, A.; Cole, A. G.; Fox, C. C.; Marsh, E. N. G. Time-resolved measurements of the photolysis and recombination of adenosylcobalamin bound to glutamate mutase. *J. Phys. Chem. B* **2005**, *109*, 18146–18152.
- (12) Sension, R. J.; Cole, A. G.; Harris, A. D.; Fox, C. C.; Woodbury, N. W.; Lin, S.; Marsh, E. N. G. Photolysis and recombination of adenosylcobalamin bound to glutamate mutase. *J. Am. Chem. Soc.* **2004**, *126*, 1598–1599.
- (13) Yoder, L. M.; Cole, A. G.; Walker, L. A.; Sension, R. J. Timeresolved spectroscopic studies of  $B_{12}$  coenzymes: Influence of solvent on the photolysis of adenosylcobalamin. *J. Phys. Chem. B* **2001**, *105*, 12180–12188.
- (14) Walker, L. A.; Shiang, J. J.; Anderson, N. A.; Pullen, S. H.; Sension, R. J. Time-resolved spectroscopic studies of B<sub>12</sub> coenzymes: The photolysis and geminate recombination of adenosylcobalamin. *J. Am. Chem. Soc.* **1998**, *120*, 7286–7292.
- (15) Mamun, A. A.; Toda, M. J.; Lodowski, P.; Kozlowski, P. M. Photolytic cleavage of Co-C bond in coenzyme  $B_{12}$ -dependent glutamate mutase. *J. Phys. Chem. B* **2019**, *123*, 2585–2598.
- (16) Yang, H.; McDaniel, E. C.; Impano, S.; Byer, A. S.; Jodts, R. J.; Yokoyama, K.; Broderick, W. E.; Broderick, J. B.; Hoffman, B. M. The elusive 5'-deoxyadenosyl radical: Captured and characterized by electron paramagnetic resonance and electron nuclear double resonance spectroscopies. J. Am. Chem. Soc. 2019, 141, 12139—12146.
- (17) Jost, M.; Simpson, J. H.; Drennan, C. L. The transcription factor CarH safeguards use of adenosylcobalamin as a light sensor by altering the photolysis products. *Biochemistry* **2015**, *54*, 3231–3234.
- (18) Kutta, R. J.; Hardman, S. J. O.; Johannissen, L. O.; Bellina, B.; Messiha, H. L.; Ortiz-Guerrero, J. M.; Elías-Arnanz, M.; Padmanabhan, S.; Barran, P.; Scrutton, N. S.; et al. The photochemical mechanism of a B<sub>12</sub>-dependent photoreceptor protein. *Nat. Commun.* **2015**, *6*, 7907.
- (19) Bridwell-Rabb, J.; Drennan, C. L. Vitamin B<sub>12</sub> in the spotlight again. *Curr. Opin. Chem. Biol.* **2017**, *37*, 63–70.
- (20) Jost, M.; Fernández-Zapata, J.; Polanco, M. C.; Ortiz-Guerrero, J. M.; Chen, P. Y. T.; Kang, G.; Padmanabhan, S.; Elías-Arnanz, M.; Drennan, C. L. Structural basis for gene regulation by a B<sub>12</sub>-dependent photoreceptor. *Nature* **2015**, *526*, *536*–541.
- (21) Toda, M. J.; Lodowski, P.; Mamun, A. A.; Jaworska, M.; Kozlowski, P. M. Photolytic properties of the biologically active forms of vitamin B<sub>12</sub>. *Coord. Chem. Rev.* **2019**, 385, 20–43.
- (22) Toda, M. J.; Mamun, A. A.; Lodowski, P.; Kozlowski, P. M. Why is CarH photolytically active in comparison to other B12-dependent enzymes? *J. Photochem. Photobiol. B, Biol.* **2020**, 209, 111919.

- (23) Mebs, S.; Henn, J.; Dittrich, B.; Paulmann, C.; Luger, P. Electron densities of three B<sub>12</sub> vitamins. *J. Phys. Chem. A* **2009**, *113*, 8366–8378.
- (24) Gruber, K.; Reitzer, R.; Kratky, C. Radical shuttling in a protein: Ribose pseudorotation controls alkyl-radical transfer in the coenzyme B<sub>12</sub> dependent enzyme glutamate mutase. *Angew. Chem., Int. Ed.* **2001**, *40*, 3377–3380.
- (25) Wiley, T. E.; Miller, N. A.; Miller, W. R.; Sofferman, D. L.; Lodowski, P.; Toda, M. J.; Jaworska, M.; Kozlowski, P. M.; Sension, R. J. Off to the races: Comparison of excited state dynamics in vitamin  $B_{12}$  derivatives hydroxocobalamin and aquocobalamin. *J. Phys. Chem.* A **2018**, *122*, 6693–6703.
- (26) Wiley, T. E.; Miller, W. R.; Miller, N. A.; Sension, R. J.; Lodowski, P.; Jaworska, M.; Kozlowski, P. M. Photostability of hydroxocobalamin: Ultrafast excited state dynamics and computational studies. *J. Phys. Chem. Lett.* **2016**, *7*, 143–147.
- (27) Shiang, J. J.; Walker, L. A.; Anderson, N. A.; Cole, A. G.; Sension, R. J. Time-resolved spectroscopic studies of  $B_{12}$  coenzymes: The photolysis of methylcobalamin is wavelength dependent. *J. Phys. Chem. B* **1999**, *103*, 10532–10539.
- (28) Cole, A. G.; Yoder, L. M.; Shiang, J. J.; Anderson, N. A.; Walker, L. A.; Banaszak Holl, M. M.; Sension, R. J. Time-resolved spectroscopic studies of  $B_{12}$  coenzymes: A comparison of the primary photolysis mechanism in methyl-, ethyl-, n-propyl-, and 5′-deoxyadenosylcobalamin. J. Am. Chem. Soc. 2002, 124, 434–441.
- (29) Chollet, M.; Alonso-Mori, R.; Cammarata, M.; Damiani, D.; Defever, J.; Delor, J. T.; Feng, Y.; Glownia, J. M.; Langton, J. B.; Nelson, S.; et al. The X-ray pump-probe instrument at the Linac Coherent Light Source. *J. Synchrotron Rad.* **2015**, 22, 503–507.
- (30) Miller, N. A.; Michocki, L. B.; Alonso-Mori, R.; Britz, A.; Deb, A.; Deponte, D. P.; Glownia, J. M.; Kaneshiro, A. K.; Kieninger, C.; Koralek, J.; et al. Antivitamins B<sub>12</sub> in a microdrop: The excited-state structure of a precious sample using transient polarized X-ray absorption near-edge structure. *J. Phys. Chem. Lett.* **2019**, *10*, 5484–5489.
- (31) Michocki, L. B.; Miller, N. A.; Alonso-Mori, R.; Britz, A.; Deb, A.; Glownia, J. M.; Kaneshiro, A. K.; Konar, A.; Koralek, J.; Meadows, J. H.; Sofferman, D. L.; et al. Probing the excited state of methylcobalamin using polarized time-resolved X-ray absorption spectroscopy. *J. Phys. Chem. B* **2019**, *123*, 6042–6048.
- (32) Miller, N. A.; Michocki, L. B.; Konar, A.; Alonso-Mori, R.; Deb, A.; Glownia, J. M.; Sofferman, D. L.; Song, S.; Kozlowski, P. M.; Kubarych, K. J.; et al. Ultrafast XANES monitors sequential structural evolution in photoexcited coenzyme B<sub>12</sub>. *J. Phys. Chem. B* **2020**, *124*, 199–209.
- (33) Stickrath, A. B.; Carroll, E. C.; Dai, X.; Harris, D. A.; Rury, A.; Smith, B.; Tang, K.-C.; Wert, J.; Sension, R. J. Solvent-dependent cage dynamics of small nonpolar radicals: Lessons from the photo-dissociation and geminate recombination of alkylcobalamins. *J. Phys. Chem. A* **2009**, *113*, 8513–8522.
- (34) Sension, R. J.; Harris, D. A.; Cole, A. G. Time-resolved spectroscopic studies of  $B_{12}$  coenzymes: A comparison of the influence of solvent on the primary photolysis mechanism and geminate recombination of methyl-, ethyl-, n-propyl-, and 5'-deoxyadenosylcobalamin. *J. Phys. Chem. B* **2005**, *109*, 21954–21962.
- (35) Walker, L. A.; Jarrett, J. T.; Anderson, N. A.; Pullen, S. H.; Matthews, R. G.; Sension, R. J. Time-resolved spectroscopic studies of  $B_{12}$  coenzymes: The identification of a metastable cob(III)alamin photoproduct in the photolysis of methylcobalamin. *J. Am. Chem. Soc.* **1998**, *120*, 3597–3603.
- (36) Harris, D. A.; Stickrath, A. B.; Carroll, E. C.; Sension, R. J. Influence of environment on the electronic structure of cob(III)-alamins: Time-resolved absorption studies of the  $S_1$  state spectrum and dynamics. *J. Am. Chem. Soc.* **2007**, *129*, 7578–7585.
- (37) Jones, A. R.; Russell, H. J.; Greetham, G. M.; Towrie, M.; Hay, S.; Scrutton, N. S. Ultrafast infrared spectral fingerprints of vitamin B<sub>12</sub> and related cobalamins. *J. Phys. Chem. A* **2012**, *116*, 5586–5594. (38) Subramanian, G.; Zhang, X.; Kodis, G.; Kong, Q.; Liu, C.; Chizmeshya, A.; Weierstall, U.; Spence, J. Direct structural and

- chemical characterization of the photolytic intermediates of methylcobalamin using time-resolved X-ray absorption spectroscopy. *J. Phys. Chem. Lett.* **2018**, *9*, 1542–1546.
- (39) Levantino, M.; Lemke, H. T.; Schiro, G.; Glownia, M.; Cupane, A.; Cammarata, M. Observing heme doming in myoglobin with femtosecond X-ray absorption spectroscopy. *Struc. Dyn.* **2015**, *2*, No. 041713.
- (40) Silatani, M.; Lima, F. A.; Penfold, T. J.; Rittmann, J.; Reinhard, M. E.; Rittmann-Frank, H. M.; Borca, C.; Grolimund, D.; Milne, C. J.; Chergui, M. NO binding kinetics in myoglobin investigated by picosecond Fe K-edge absorption spectroscopy. *Proc. Natl. Acad. Sci. U. S. A.* **2015**, *112*, 12922–12927.
- (41) Mara, M. W.; Hadt, R. G.; Reinhard, M. E.; Kroll, T.; Lim, H.; Hartsock, R. W.; Alonso-Mori, R.; Chollet, M.; Glownia, J. M.; Nelson, S.; et al. Metalloprotein entatic control of ligand-metal bonds quantified by ultrafast x-ray spectroscopy. *Science* **2017**, 356, 1276–1280
- (42) Chatterjee, R.; Weninger, C.; Loukianov, A.; Gul, S.; Fuller, F. D.; Cheah, M. H.; Fransson, T.; Pham, C. C.; Nelson, S.; Song, S.; et al. XANES and EXAFS of dilute solutions of transition metals at XFELs. *J. Synchrot. Radiat.* **2019**, *26*, 1716–1724.
- (43) Shelby, M. L.; Lestrange, P. J.; Jackson, N. E.; Haldrup, K.; Mara, M. W.; Stickrath, A. B.; Zhu, D.; Lemke, H. T.; Chollet, M.; Hoffman, B. M.; et al. Ultrafast excited state relaxation of a metalloporphyrin revealed by femtosecond X-ray absorption spectroscopy. J. Am. Chem. Soc. 2016, 138, 8752–8764.
- (44) Miller, N. A.; Deb, A.; Alonso-Mori, R.; Garabato, B. D.; Glownia, J. M.; Kiefer, L. M.; Koralek, J.; Sikorski, M.; Spears, K. G.; Wiley, T. E.; et al. Polarized XANES monitors femtosecond structural evolution of photoexcited vitamin B<sub>12</sub>. *J. Am. Chem. Soc.* **2017**, *139*, 1894–1899.
- (45) Miller, N. A.; Deb, A.; Alonso-Mori, R.; Glownia, J. M.; Kiefer, L. M.; Konar, A.; Michocki, L. B.; Sikorski, M.; Sofferman, D. L.; Song, S.; et al. Ultrafast X-ray absorption near edge structure reveals ballistic excited state structural dynamics. *J. Phys. Chem. A* **2018**, *122*, 4963–4971.
- (46) Sarkar, S.; Witham, S.; Zhang, J.; Zhenirovskyy, M.; Rocchia, W.; Alexov, E. DelPhi web server: A comprehensive online suite for electrostatic calculations of biological macromolecules and their complexes. *Commun. Comput. Phys.* **2013**, *13*, 269–284.
- (47) Smith, N.; Witham, S.; Sarkar, S.; Zhang, J.; Li, L.; Li, C.; Alexov, E. DelPhi web server v2: incorporating atomic-style geometrical figures into the computational protocol. *Bioinformatics* **2012**, 28, 1655–1657.